XVIII[èmes] Journées Nationales Génie Côtier – Génie Civil
Anglet, 2024
DOI:10.5150/jngcgc.2024.056 *© Editions Paralia CFL*
disponible en ligne – http://www.paralia.fr – available online

Parametric study to derive wave patterns and bathymetry on synthetic waves

Alisson VILLCA [1], Adrien POUPARDIN [1], Muhammad Ali SAMMUNEH [1], Jena JEONG [1], Georges CHAPALAIN [2]

1. Université Paris-Est, Institute de Recherche en Construction, 28 Av. du Président Wilson, 94230 Cachan, France.
   apoupardin@estp.fr
2. Cerema Risques Eau Mer, Margny-Lès-Compiègne, 60280, France.
   Georges.Chapalain @cerema.fr

Abstract:
The knowledge of regional bathymetry is crucial for assessing the effects of climate change. Remote sensing techniques play an important role in extracting intermediate bathymetric data across large areas, because of the frequent revisit times of satellites. Utilizing satellite-derived bathymetry, which harnesses optical imagery from satellite missions such as Sentinel-2, presents a cost-effective complement to traditional *in-situ* surveys. This study introduces a refined approach, building upon an existing method that uses wavelet and cross correlation techniques to derive bathymetry solely from a pair of images with a time lag thus eliminating the need for *in-situ* measurements. By analysing synthetic images using sub-pixel registration instead of cross correlation, the method achieves enhanced accuracy. To assess the impact of resolution and the expected errors in bathymetry different collections of synthetic images with varying resolutions are analyzed. The effectiveness of enhancing wave patterns through the radon transform is also examined and its results compared to images which displacement was calculated by cross-correlation and dft-registration.

Keywords:
Bathymetry inversion, Synthetic waves, Wavelet, Celerity, Radon transform.

1. Introduction

Storm events drive substantial sediment transport, causing rapid erosion, while recovery during calm periods is slower. Recognizing these dynamics is essential for predicting wave behavior accurately. Due to climate change coastal regions face a double threat increased storm intensity and sea level rise (PÖRTNER *et al.*, 2022, 2023). Understanding dynamic coastal bathymetry is crucial for effective environmental management and climate change mitigation strategies.

As a low cost complement to *in-situ* surveys satellite images provide valuable data, frequently employed in algorithms to estimate near-shore bathymetry in un-surveyed areas (ELLIS *et al.*, n.d.). A straightforward approach uses reflectance values of different bands where the depth is related to the height of the water column, this means the darker the colour the deeper the depth. Among the most used methods to estimate bathymetry, which rely on *in-situ* data, are the linear transform (LYZENGA, 1978) and the ratio transform (STUMPF *et al.*, 2003) methods that require the tuning of five and two parameters respectively. These methods have proven to be reliable for bathymetry estimation for depths <20m in turbidity free water images. In cases of high turbidity areas some variations of these methods have been used (LIANG *et al.*, 2024); One notable advantage is that the estimated bathymetry maintains the resolution of the bands used. However, a drawback is that it necessitates *in-situ* data for calibration.

To circumvent the dependency on *in-situ* data, inversion methods leveraging on wave celerity and wavelength estimation are often employed, enabling the retrieval of local water depth. These have been used in optical images (POUPARDIN *et al.*, 2016; DE MICHELE *et al.*, 2021) to retrieve bathymetry for intermediate depths. One limitation of water depth inversion methods is that waves have to be clearly visible on the images; solar reflections can be useful for spatially locating wave crests. The proper combination of the solar elevation angle E and the viewing incidence angle I can provide an assessment of image quality, with the condition $60 < E+I < 120$ (POPULUS *et al.*, 1991). Another limitation is that the resolution of the resultant estimated bathymetry map is lower (between 200m and 50m) compared to the bands utilized for its derivation. The time lag between bands is variable, for example Sentinel-2 time-lag varies between 0.986s and 1.025s for blue (B2) and red (B4) bands it can affect the depth error up to 10% according to BINET *et al.*, (2022). However we will use a fixed time lag of 1.005s for our synthetic images. The image resolution and time step can determine whether one can effectively detect and measure the wave phase. The lower the resolution the less likely is to detect the shorter wavelengths (resolution $< 0.5\ \lambda$).

This study aims to test the limits of the cross-correlation wavelet bathymetry method (POUPARDIN *et al.*, 2016) on a collection of synthetic images with variable periods and wavelengths (T, λ) for intermediate depths to assess the effect of the various resolutions from 10m, to 5m and 2.5m using dft registration for the displacement calculation, with the intention of enhancing the Sentinel-2 images a collection of radon filtered 10m

resolution synthetic images is also tested and its results compared to images whose displacement was calculated by cross-correlation and dft-registration.

2. Methodology

Most water depth inversion methods rely on the dispersion relation based on the linear wave theory in case the wave is propagating through shallow to intermediate waters (i.e. λ/20 < h < λ/2).

$$h = \frac{\lambda}{2\pi}\tanh^{-1}\left(\frac{2\pi c^2}{g\lambda}\right) \quad (1)$$

where h is water depth, λ is wavelength, c is celerity or phase velocity and g is the gravitational acceleration. The methodological process can be separated in 4 steps, (1) determine the parameters of the wave, wavelength and wave direction in a couple of images, (2) determine the displacement the wave underwent in that direction during the time step, (3) approximate the celerity and (4) water depth calculation through the fitting of the dispersion equation with a cloud of wavelengths and celerities. Spatial wave characteristics such as wavelength and propagation direction (λ, θ) can be derived from space born imagery using wavelet analysis. The Morlet wavelets are shifted, rotated and scaled to detect waves. The aim is to estimate the displacement of wave crests between bands (POUPARDIN *et al*., 2016) but instead of using cross correlation to estimate the displacement the sub pixel image registration method is used *(GUIZAR-SICAIROS et al.*, 2008). This will result in more precise estimations of wave displacement and thus celerity.

3. Radon transform

Predominantly used for tomography, astronomy and microscopy. The radon transform is commonly used in the detection of lines in digital images and is able to enhance linear features (TOFT, 1996). The radon transform $g\check{}(\rho,\theta)$ of a continuous two dimensional function $g(x,y)$ is found integrating said function along slanted lines (in its normal form $\rho = xcos\theta + ysin\theta$). A key property is that a line in an image is transformed into a peak in the parameter domain (θ,ρ), where the position of the peak corresponds to the line parameters.

$$g\check{}(\rho,\theta) = \iint g(x,y)\,\delta(\rho - x\cos\theta - y\sin\theta)dxdy \quad (2)$$

where δ represents the Dirac delta function, and $g\check{}(\rho,\theta)$ the radon transform also called the sinogram. All lines can be described choosing $0 < \theta < 2\pi$ and $\rho \geq 0$. Once the sinogram has been calculated the image can be reconstructed by the inverse of the radon transform.

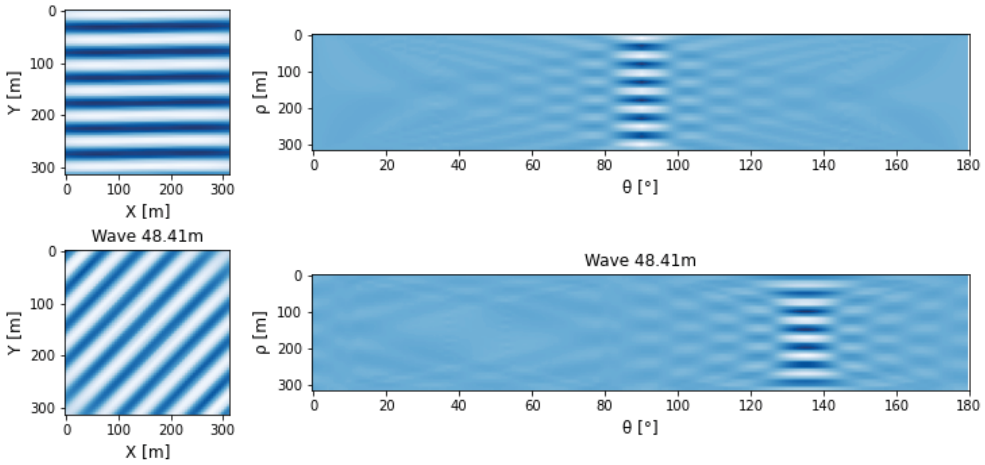

Figure 1. Radon filtered synthetic sinusoidal waves (from the 10m waves in Figure 2), and corresponding sinograms for wave propagation direction 90° degrees and 135° degrees.

Sentinel-2 wave features can be improved by radon filtering and reconstruction over a limited number of angles, the main wave propagation direction, after increasing the sinogram resolution by image augmentation (BERGSMA *et al*., 2019). In this study we will assess the impact of this pre-processing step in our synthetic wave image collection. In Figure 2 the 10m resolution images are shown and in Figure 1 the radon filtered 5m resolution images, the wave features already improved, and next to them the sinograms that were used to derive them, with angles between the main wave propagation direction angles (80° to 100°) for the upper left image and (125° to 145°) for the lower left image.

4. Synthetic waves for intermediate water depths

To study the impact of varying resolutions on the bathymetry estimation synthetic waves are generated for periods between 6 and 10s in three different resolutions 10m, 5m, and 2.5m with a time step of 1.005s (see Figure 2). The amplitude for the sinusoidal wave is 1m, the wave number $k = 2\pi/\lambda$, the angular frequency $\omega=2\pi/T$. Another set of synthetic waves was generated with resolution of 10m in order to compare three different approaches. The first, use cross-correlation to calculate displacements with an initial resize of 4, use dft registration to calculate displacements with no resize or pre-processing done and the third, use radon filtered images with a resize 2 for the sinogram and dft registration. The window size is variable depending on the wavelength detected keeping at least three troughs and three crests for every sub dataset. For every synthetic image a single representative value of displacement and bathymetry are then plotted.

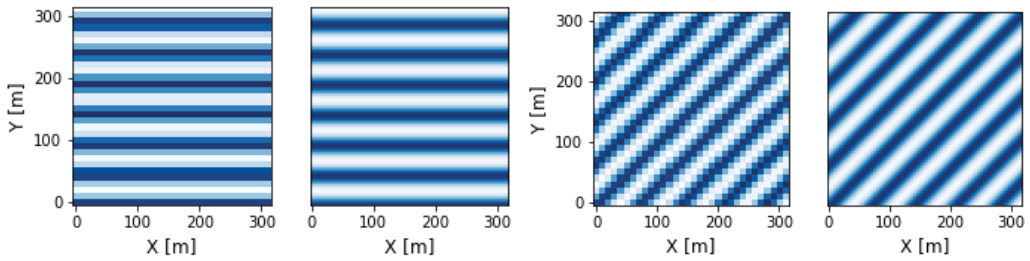

Figure 2. Synthetic sinusoidal waves, wave propagation a) direction 90°degrees and b) 135° degrees for 10m and 5m resolution.

5. Results and discussion

The improvement brought about by sub-pixel registration is more evident when comparing the displacement error interval from Figures 3a, 4a and 5a. When using the cross-correlation method displacements are at a pixel level, whereas when using dft registration the displacements are in a sub-pixel level this is the reason why displacement approximation is improved from a [+17.2%,-9.4%] interval to [+7.6%,-15.6%]. For the radon filtered images this range is [+7.8%,-1.2%]. It's crucial to highlight that this enhancement represents a significant improvement in estimating wave celerity. We must bear in mind that the CWB method is particularly sensitive to changes in celerity (POUPARDIN *et al.*, 2016). Bathymetry estimates also significantly improve following the radon filter preprocessing steps (see Figure 6).

In the implementation of dft registration to calculate inter-band displacement an issue emerged. Occasional displacements in the opposite direction were observed when using dft registration instead of cross correlation; this led to general underestimation of water depth. After assuming that all waves in a sub dataset are propagating in the same direction the uniformity on the celerity field was possible, thus discarding all displacement that do not agree with the main direction of wave propagation.

Overall for every sub dataset the wavelengths are very well approximated and its values are almost uniform, the same happens with the displacement and celerity fields. But by the time the depth inversion is done small variations in celerity values affect the calculated bathymetry value leading in the majority of cases to underestimation of depth, the error increases the more we approach deeper values. This is because we use the dispersion equation, a point is reached were wavelengths are similar and celerity governs bathymetry. For low wave periods as 6s or 7s we reach this plateau where even dft registration struggles to detect displacements accurately enough, bathymetry underestimation is quite important in 10m resolution images (see Figure 4c).

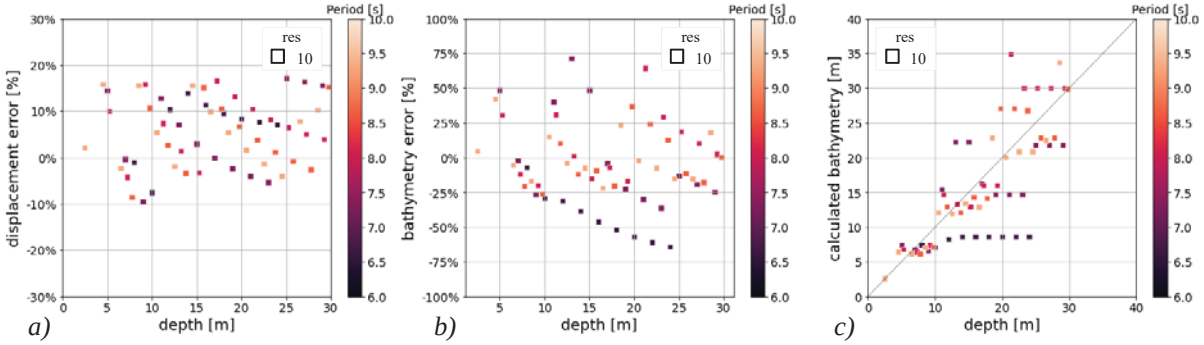

a) *b)* *c)*

*Figure 3. Bathymetry and displacement error per depth through **cross-correlation.***
a) Displacement error variation with depth, b) Bathymetry error variation with depth, c) calculated bathymetry versus depth. Results are shown for initial resolution of 10m. Previous resize of 4 is done.

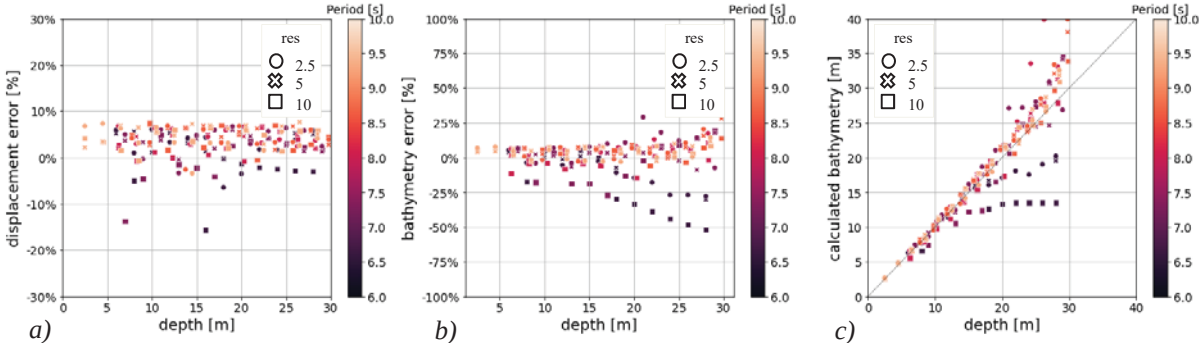

a) *b)* *c)*

*Figure 4. Bathymetry and displacement error per depth through **dft-registration.***
a) Displacement error variation with depth, b) Bathymetry error variation with depth, c) calculated bathymetry versus depth. Results are shown for resolutions 10, 5and 2.5m.

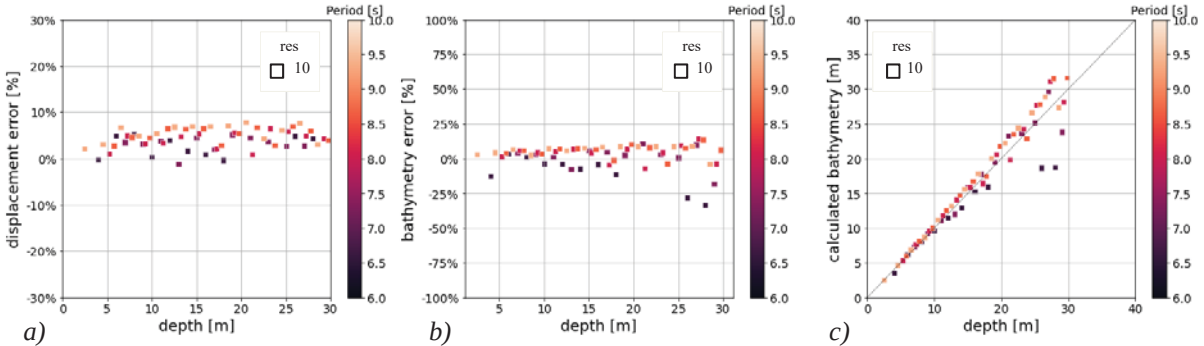

a) *b)* *c)*

*Figure 5. Bathymetry and displacement error per depth through **radon filter and dft registration**. a) Displacement error variation with depth, b) Bathymetry error variation with depth, c) calculated bathymetry versus depth. Results are shown for initial resolution of 10m which sinogram resolution was augmented by a factor of 2.*

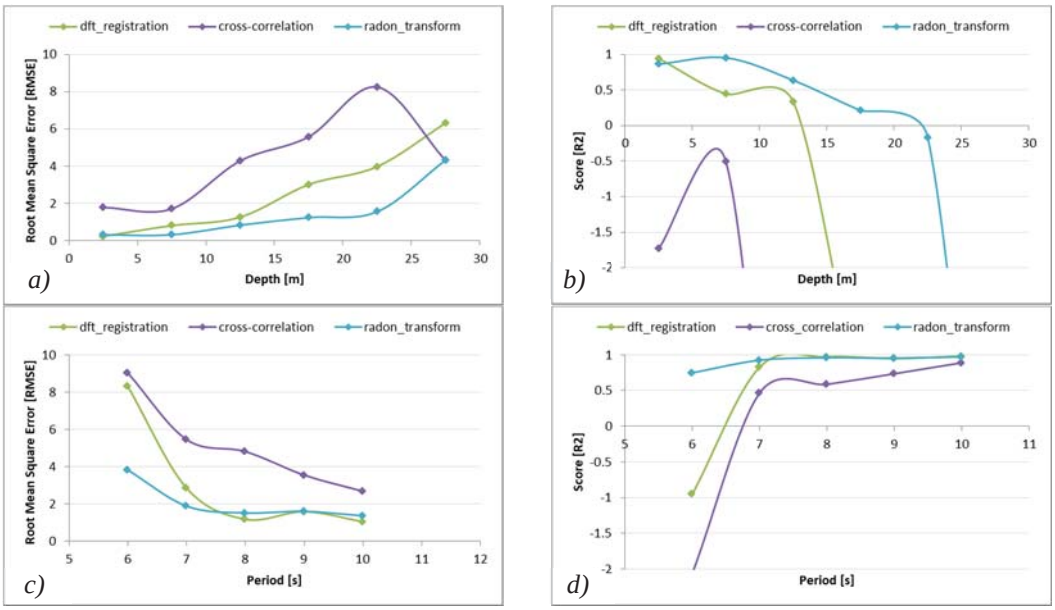

Figure 6. RMSE error comparison and bathymetry accuracy (R^2) between cross-correlation, dft-registration and radon transform, varying with depth (a and b), and varying with wave period (c and d). Initial resolution for all cases is 10m.

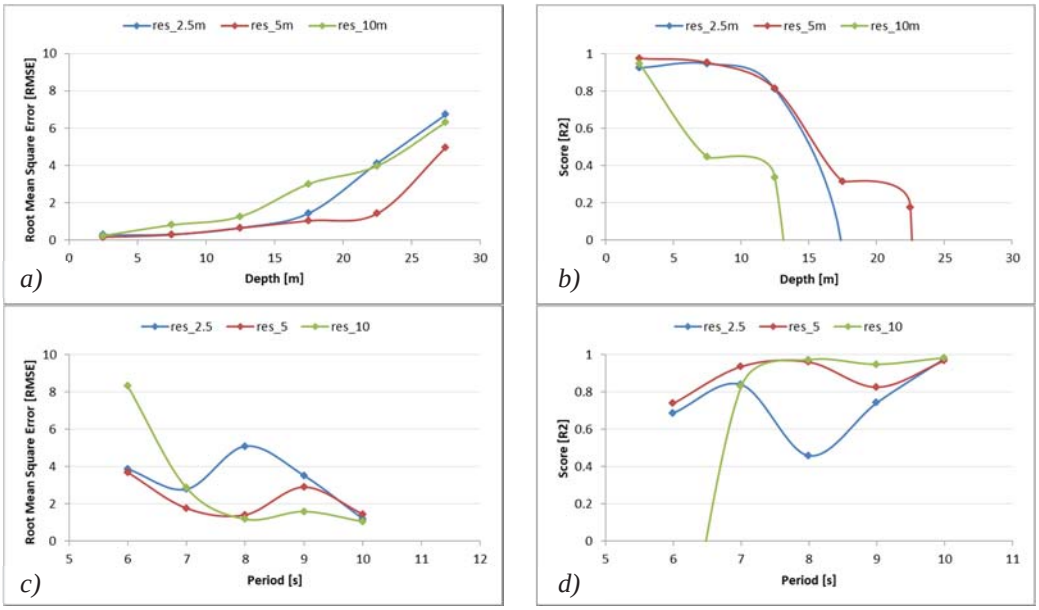

Figure 7. RMSE error comparison and bathymetry accuracy (R^2) comparison for resolutions 10, 5 and 2.5m using dft-registration, varying with depth (a and b), and varying with wave period (c and d).

Most satellite derived bathymetry studies show the accuracy of their results in terms of root mean square error (RMSE) and determination coefficient (R^2).

$$RMSE = \sqrt{\frac{1}{N}\sum_{i=1}^{N}(y_i - \hat{y})^2} \quad (3)$$

$$R^2 = 1 - \frac{\sum_{i=1}^{N}(y_i - \hat{y})^2}{\sum_{i=1}^{N}(y_i - \bar{y})^2} \quad (4)$$

where, y_i is the actual value $\hat{y}$ is the predicted value, $\bar{y}$ is the mean y_i values and N is the number of observations. So let's see first the impact of our three different approaches, every RMSE and R^2 value is calculated for 5m depths interval. From Figures 6a in terms of RMSE the best performance for all depth intervals is for the radon filtered images, on the contrary cross correlation gives the worst performance. In terms of R^2, (Figure 6b) cross-correlation does not perform well in any depth interval while dft-registration performance declines severely for depths >15m, and for radon-filtered images the same decline is observed for depths >20m. By considering RMSE and R^2 this time (Figure 6c and 6d) for waves of same periods where every RMSE and R^2 value is calculated for all waves with the same wave period, we can see the error is higher for low period waves.
Regarding the impact of image resolution on the estimated bathymetry from Figure 7a is the 5m resolution collection gives the best performance in terms of RMSE and R^2. Still a marked decline is seen in score values for depths >10, >15, >20m for resolutions 10, 2.5 and 5 respectively. Figures 7b and 7c show that the lowest wave period gives highest RMSE and lowest R^2 values respectively.

6. Conclusion and way forward

Importantly, this study aims to investigate the influence of various parameters on water depth estimation using CWB method under specific conditions of interest. Bathymetries were estimated for depths up to 30m, for three resolutions the best approximations are between 0-15m (RMSE<0.65) for the 5m resolution images, we introduce an alternative method for measuring displacement between bands, dft registration, that improved the estimation. Additionally, we demonstrate the enhancement in bathymetry estimation resulting from the application of a pre-processing step on 10m resolution synthetic images, wave features are enhanced using the radon filter 0-20m (RMSE<1.23). Moving forward, our goal is to utilize the CWB method on Sentinel-2 10m resolution blue (B2) and red (B4) bands in our area of study, Camargue. By incorporating variable window size and radon filtering, we anticipate achieving a maximum RMSE value of 1.23m for water depths <20m.

7. References

BERGSMA E.W.J., ALMAR R., MAISONGRANDE P. (2019). *Radon-augmented Sentinel-2 satellite imagery to derive wave-patterns and regional bathymetry*. Remote Sensing, *11*(16), 1918. https://doi.org/10.3390/rs11161918

BINET R., BERGSMA E., POULAIN V. (2022). *Accurate Sentinel-2 inter-band time delays*. ISPRS Annals of the Photogrammetry, Remote Sensing and Spatial Information Sciences, V-1–2022, 57–66. https://doi.org/10.5194/isprs-annals-V-1-2022-57-2022

DE MICHELE M., RAUCOULES D., IDIER D., SMAI F., FOUMELIS M. (2021). *Shallow bathymetry from multiple Sentinel 2 Images via the joint estimation of wave celerity and wavelength*. Remote Sensing, 13(11), Article 11. https://doi.org/10.3390/rs13112149

ELLIS M., FORMANEK R., TOWNSEND N. (n.d.). *Satellite derived bathymetry*.

GUIZAR-SICAIROS M., THURMAN S.T., FIENUP, J.R. (2008). *Efficient subpixel image registration algorithms.* Optics Letters, *33*(2), Article 2. https://doi.org/10.1364/OL.33.000156

LIANG Y., CHENG Z., DU Y., SONG D., YOU Z. (2024). *An improved method for water depth mapping in turbid waters based on a machine learning model*. Estuarine, Coastal and Shelf Science, 296, 108577. https://doi.org/10.1016/j.ecss.2023.108577

LYZENGA D.R. (1978). *Passive remote sensing techniques for mapping water depth and bottom features*. Applied Optics, 17(3), Article 3. https://doi.org/10.1364/AO.17.000379

POPULUS J., ARISTAGHES C., JONSSON L., AUGUSTIN J.M., POULIQUEN E. (1991). *The use of SPOT data for wave analysis.* Remote Sensing of Environment, 36(1), 55–65. https://doi.org/10.1016/0034-4257(91)90030-A

PÖRTNER *et al.*, 2022. (2023). *Climate Change 2022 – Impacts, Adaptation and Vulnerability: Working Group II Contribution to the Sixth Assessment Report of the Intergovernmental Panel on Climate Change (1st ed.).* Cambridge University Press. https://doi.org/10.1017/9781009325844

POUPARDIN A., IDIER D., DE MICHELE M., RAUCOULES D. (2016). *Water depth inversion from a single SPOT-5 dataset*. IEEE Transactions on Geoscience and Remote Sensing, 54(4), Article 4. https://doi.org/10.1109/TGRS.2015.2499379

STUMPF R.P., HOLDERIED K., SINCLAIR M. (2003). Determination of water depth with high-resolution satellite imagery over variable bottom types. *Limnology and Oceanography*, *48*(1part2), 547–556. https://doi.org/10.4319/lo.2003.48.1_part_2.0547

TOFT, P. (1996). *The Radon Transform—Theory and Implementation*.